

# Design of Structural Parameters of Photonic Crystal Fibers for Optimization of Dispersion Flattening Management Using FDTD Method

Faramarz E. Seraji<sup>1,\*</sup>, M. Nouri<sup>2</sup>

<sup>1</sup>Optical Communication Group, Iran Telecom Research Center, Tehran, Iran

<sup>2</sup>Elect. and Computer Eng. Dept, Science and Research Branch, Islamic Azad University, Tehran, Iran

**Abstract** In this paper, optimization and management of dispersion of photonic crystal fibers (PCF) are presented, using 2D finite difference method in time domain based on an Intelligent Programming. In the analysis, for the proposed PCF structures, by evaluation of the effective refractive indices, the dispersions are calculated for 11 circular air-hole rings in the cladding. The effects of geometrical parameters of the PCFs, such as air-hole diameters, the pitch value, number of air rings on dispersion are investigated for the influence of the structural parameters of the PCFs on the obtained dispersions and the corresponding results are graphically compared. It is shown that when the air-hole diameter decreases, the slope of the negative dispersion would increase, while increase of the pitch would cause a decrease in the negative dispersion values. It is further shown that at pitches of higher than 5  $\mu\text{m}$ , irrespective of air-hole diameter, the variation of the dispersion is almost linear. The results presented can help in choosing the PCF parameters for appropriate applications.

**Keywords** Dispersion management, Photonic crystal fibers, Optimization, FDTD

## 1. Introduction

In the past two decades, photonic crystal fibers (PCFs) have become popular for applications in designs of optical devices used in optical communication networks [1, 2] and sensing systems [3]. The particular application, which is widely used, is in designing of dispersion compensators commonly utilized in WDM optical communication networks to reduce the number of required repeaters [4, 5]. One of the characteristic features of the PCFs in comparison with conventional optical fibers is flexibilities of their characteristic parameters in response to dispersion effects on propagating pulses caused intrinsically by optical fibers in a long-haul transmission optical line [6, 7].

Several designs of dispersion compensating fibers (DCF) have been optimized for compensation of the dispersions using PCFs in optical transmission bands ranging from 1460 nm to 1675 nm [8-10]. Xuyou Li et al reported design of a pentagonal PCF with large flattened negative dispersion by using the full vector finite element method (FEM) [11]. The reported average negative dispersions for two kinds of optimized designs were  $-611.9$  ps/nm/km over

1,460–1,625 nm and  $-474$  ps/nm/km over 1425–1675 nm wavelength bands, respectively.

Raonaqul Islam et al reported design of a porous-core circular photonic crystal fiber with circular arrangement of air holes, both in the periodic cladding and the porous core [12]. The simulation results, by using an efficient finite element method, showed a flattened dispersion of  $\pm 0.09$  ps/THz/cm within the frequency range of 0.9 to 1.3 THz.

The management of the chromatic dispersion, which is achieved by doping the core of a PCF doped with Germanium was reported [13]. An ultra-flattened dispersion with a range of values from  $-210$  ps/nm.km up to  $15$  ps/nm.km was obtained. In another report, a design of a hybrid PCF with elliptical and circular air holes of hexagonal layout with triangular lattice of five rings around the solid core was presented by Varshali Sharma et al [14]. The obtained large flattened dispersion was of the order of  $4.88$  ps/nm/km for the wavelength range of 1.2 to 1.8  $\mu\text{m}$ .

In this paper, using two-dimensional finite difference time domain (2D-FDTD), three PCF structures are proposed to optimize the dispersions by considering the effects of the geometrical parameters, such as air-hole diameters and the center-to-center spacing between the holes (pitch). The air-holes are arranged in the cladding in the form of triangular lattice by constituting 11 rings around the core [15].

\* Corresponding author:

feseraji@itrc.ac.ir (Faramarz E. Seraji)

Published online at <http://journal.sapub.org/optics>

Copyright © 2017 Scientific & Academic Publishing. All Rights Reserved

## 2. Dispersion and Index Formulations

Total dispersion in an optical fiber is expressed as follows:

$$D_T = D_M + D_W \tag{1}$$

where  $D_M$  is the material dispersion and  $D_W$  indicates the waveguide dispersion that are expressed, respectively, as:

$$D_M = -(\lambda^2 / 2\pi c) \frac{d^2\beta}{d\lambda^2} \tag{2}$$

$$D_W = -(\lambda / \pi c) \frac{d\beta}{d\lambda} \tag{3}$$

where  $c$  represents the velocity of light in a vacuum,  $\lambda$  is the wavelength, and  $\beta$  indicates the propagation constant, which is defined as follows:

$$\beta(\lambda) = \sum_{i=0}^n a_i \lambda^i \tag{4}$$

where  $\lambda^i$  is the operating wavelength,  $a_i$  a constant coefficient, and  $n$  is a natural number. For evaluation of the dependency of refractive index of silica on wavelength, the Sellmeier formula is used, which is defined as follows:

$$n_s^2 = 1 + \sum_{i=1}^3 \frac{S_i \lambda^2}{\lambda^2 - L_i^2} \tag{5}$$

where  $S_i$  represents the coefficients related to the strength of material oscillator and  $L_i$  denotes the corresponding wavelength of the oscillator. Finally, the effective refractive index  $n_{eff}$  is determined with respect to the structural parameters of the PCFs, using the following approximate expression [10]:

$$n_{eff}(\lambda) = n_a \frac{(d/\Lambda)N}{0.5d/\Lambda + N} + n_s(\lambda) \frac{(1-d/\Lambda)N + 0.5d/\Lambda}{0.5d/\Lambda + N} \tag{6}$$

The above expression suitably establishes the relationship between  $n_{eff}$  and air-hole diameter  $d$ , the number of air rings in the cladding  $N$ , and the pitch  $\Lambda$  with effective refractive indices of the core  $n_s$  and air  $n_a$ .

## 3. Design of the PCFs for Dispersion Management

### 3.1. Design Procedures

The dispersion analysis is performed by considering the variations of the air-hole diameter and the pitch in a PCF of 11 air-hole rings in the cladding. At the first stage of the analysis, the shapes of all the air-holes in the 11 rings are circular arranged in triangular lattice with equal diameters of  $0.75\mu\text{m}$  and the pitch ( $\Lambda$ ) is  $2\mu\text{m}$ .

By using 2d-FDTD method, the cross-section, effective refractive index, and dispersion as a function of wavelength

are depicted in Fig. 1. The variations of the dispersion in the wavelength range of  $0.8\mu\text{m}$  to  $1.8\mu\text{m}$  are obtained from  $-70$  to  $+22$  ps/nm.km. The dispersion values at  $1300\text{nm}$  and  $1550\text{nm}$  are zero and about  $14$  ps/nm.km, respectively, with a mild changing slope. In another attempt, based on the intelligent algorithm [10], by further increase of the air-hole diameter to  $d=1.19\mu\text{m}$ , while keeping the pitch  $\Lambda = 2\mu\text{m}$ , it is noticed that the variations of the dispersion has changed from  $-47$  to  $+15$  ps/nm.km and the value at  $1.55\mu\text{m}$  is obtained at about  $9$  ps/nm.km, as shown in Fig. 2. That is, by increasing the air-hole diameter by about  $37\%$ , there will be a reduction of dispersion value of  $36\%$  (5 units) smaller than the previous case.

The dispersion slope at  $1.55\mu\text{m}$  in second case (Fig. 2) is  $3.64$  deg. higher than that of the first case (Fig. 1). In the final stage of design procedure, the impact of large variations of the pitch  $\Lambda = 10\mu\text{m}$  on the dispersion property is investigated for air-hole diameter of  $d = 0.75\mu\text{m}$ . The corresponding numerical results are graphically depicted in Fig. 3. Noteworthy to mention that by sudden increase of the pitch, the PCF structure is not rumbled and the holes arrangement is taken care by the employed intelligent algorithm [10].

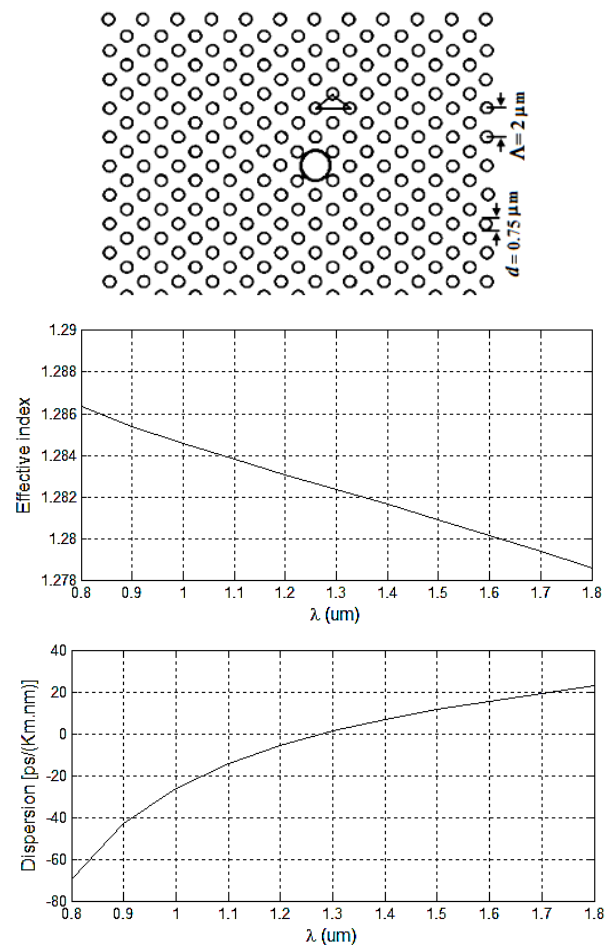


**Figure 1.** Cross-section of PCF with  $\Lambda = 2\mu\text{m}$ ,  $d = 0.75\mu\text{m}$ ,  $N = 11$  (Above), the effective refractive index (Middle), and dispersion (Below) as functions of wavelength

**3.2. Impact of Geometrical Parameters of PCFs**

More investigations on impact of geometrical parameters of designed PCFs are carried out by considering different values of the air-hole diameter and the pitch  $\Lambda$  values.

The first attempt was on increasing the air-hole diameter in a range of  $d = 0.75 \mu\text{m}$  to  $d = 1.85 \mu\text{m}$  with constant pitch of  $\Lambda = 2 \mu\text{m}$  and number of air-hole ring  $N = 11$ . The numerical results of dispersion variations in terms of wavelength are illustrated in Fig. 4 [16]. We note that for the given value of  $\Lambda$ , over calculating range of the wavelength, when air-hole diameter increases, the slope of the dispersion would decrease and becomes more flattened.

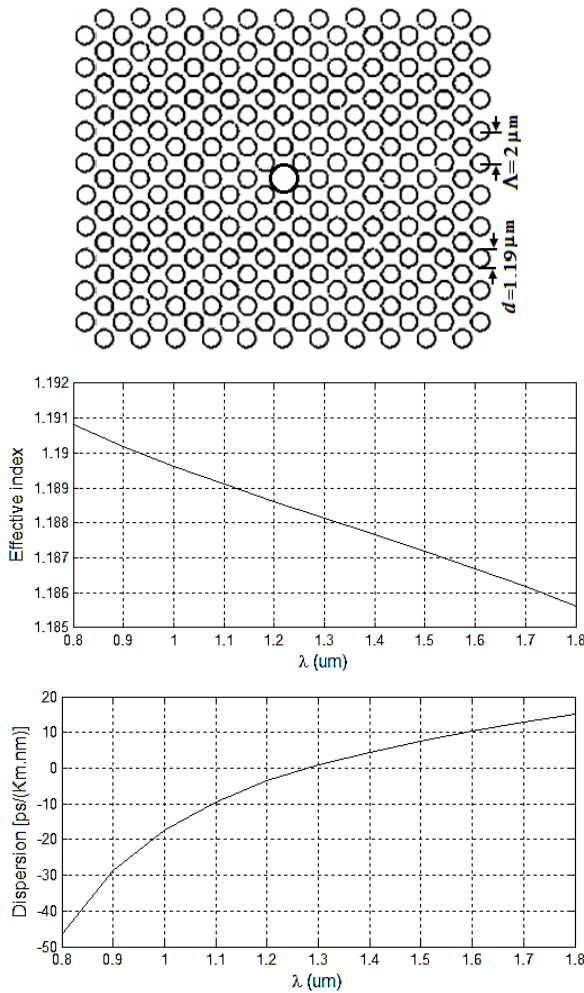


**Figure 2.** Cross-section of PCF with  $\Lambda = 2 \mu\text{m}$ ,  $d = 1.19 \mu\text{m}$ ,  $N = 11$  (Above), the effective refractive index (Middle), and the dispersion (Below) as functions of wavelength

For the typical given range of air-hole diameter from  $d = 0.75 \mu\text{m}$  to  $d = 1.85 \mu\text{m}$ , the variations of the dispersion slope versus air-hole diameter is plotted in Fig. 5, where the pitch  $\Lambda = 2 \mu\text{m}$  and the number of air-hole ring  $N = 11$ . It is observed that when the air-hole diameter increases, the slope at  $1.55 \mu\text{m}$  would decrease to the lowest level for a typical maximum value of  $d = 1.85 \mu\text{m}$ . It shows that the trend of dispersion slope variations in terms of

air-hole diameter is almost linear. As  $d$  increases, the dispersion in the wavelength range of  $1.3 \mu\text{m}$  to  $1.8 \mu\text{m}$ , becomes more flat [8, 17].

On the other hand, the impact of the pitch on the dispersion in a range of  $\Lambda = 1.5 \mu\text{m}$  to  $\Lambda = 10 \mu\text{m}$  with respect to wavelength is investigated, by considering two separate values of air-hole diameter of  $d = 0.75 \mu\text{m}$  and  $d = 1.85 \mu\text{m}$ .

The numerical results are illustrated in Fig. 6. In comparison to Fig. 4, it is noticed that as the pitch increases, the tail of the dispersion curve tends to more negative levels in shorter wavelengths, while in longer wavelengths, the dispersions become more positive. This condition is observed for both values of the air-hole diameter.

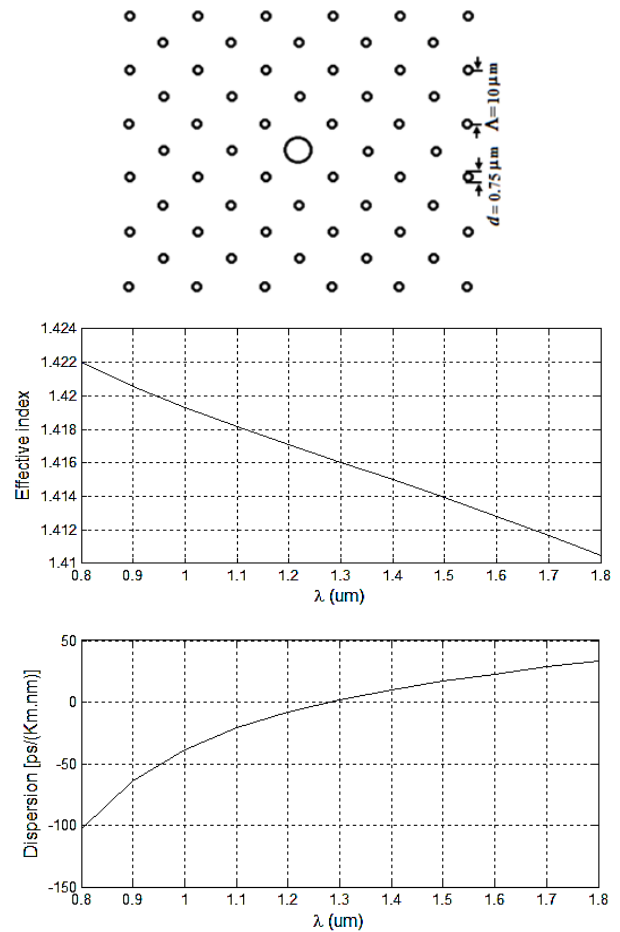


**Figure 3.** As previous curves for  $\Lambda = 10 \mu\text{m}$ ,  $d = 0.75 \mu\text{m}$ , and  $N = 11$

The distinguishable difference between Figs. 6a and 6b is derived mainly from the influence of changes of the air-hole diameter  $d$ . When  $d$  increases, the slope of the dispersion curve would reduce and tends to a flatter levels [9]. In general, as  $d$  decreases, the dispersion slope would increase, whereas an increase in the pitch would cause the dispersion slope to increase. Therefore, the impacts of air-hole diameter  $d$  and the pitch  $\Lambda$  counterbalance each other.

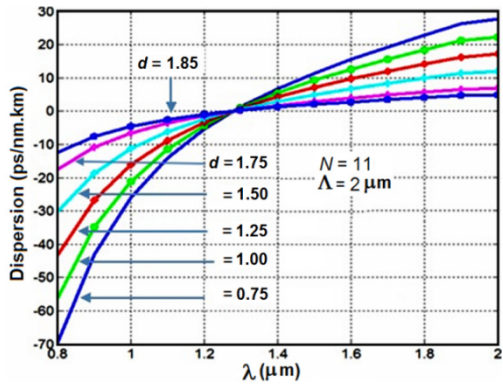


**Figure 4.** Dispersion versus wavelength for different values of the air-hole diameter,  $\Lambda = 2 \mu\text{m}$ , and  $N = 11$

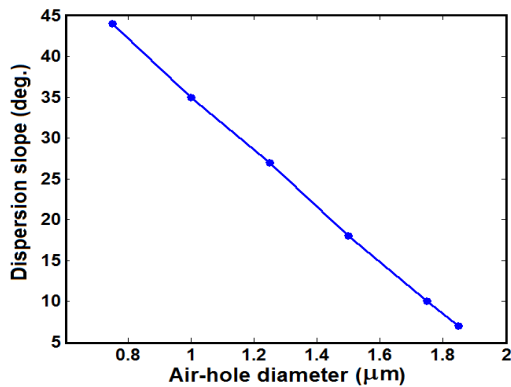


**Figure 5.** Variation of the dispersion slope versus air-hole diameters for  $\Lambda = 2 \mu\text{m}$  and  $N = 11$

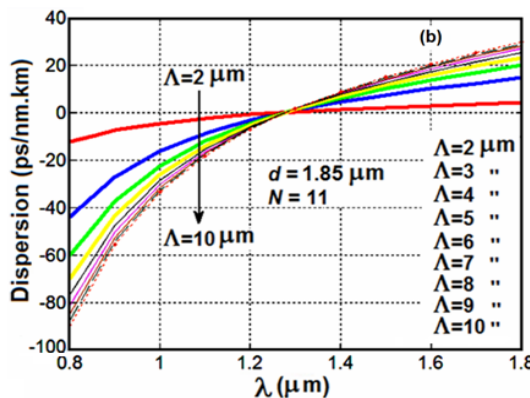
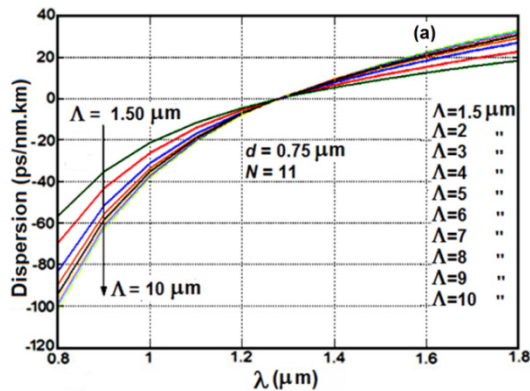


**Figure 6.** Dispersion versus wavelength for different values of the pitch for (a)  $d = 0.75 \mu\text{m}$ , (b)  $d = 1.85 \mu\text{m}$ , and  $N = 11$

More investigations are carried out on parametric effects on the variations of the dispersion towards optimization of the proposed designs of PCFs. At this stage, the variations of the dispersion are studied with respect to the pitch at two wavelengths  $0.8 \mu\text{m}$  and  $1.55 \mu\text{m}$  for various values of the air-hole diameter  $d$ , as depicted in Figs. 7.

If we compare two Figs. 7a and 7b, it's noted that in the calculating range of the pitch  $\Lambda$ , the dispersion values exponentially become more negative at wavelength  $0.8 \mu\text{m}$ , while at higher wavelength  $1.55 \mu\text{m}$ , the changing trend of the dispersion is towards positive values. At the same time, the impact of the variations in air-hole diameter  $d$ , causes different changes for two wavelengths. At  $d = 0.75 \mu\text{m}$  and  $\lambda = 1.55 \mu\text{m}$ , the dispersion variations is about  $+5.15 \text{ ps/nm.km}$ , whereas at  $\lambda = 0.80 \mu\text{m}$  with the same value of  $d$ , the variation is about  $-27 \text{ ps/nm.km}$ .

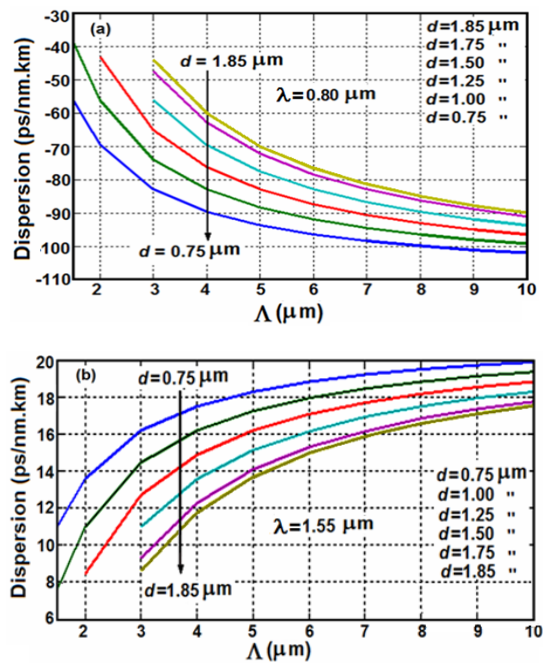


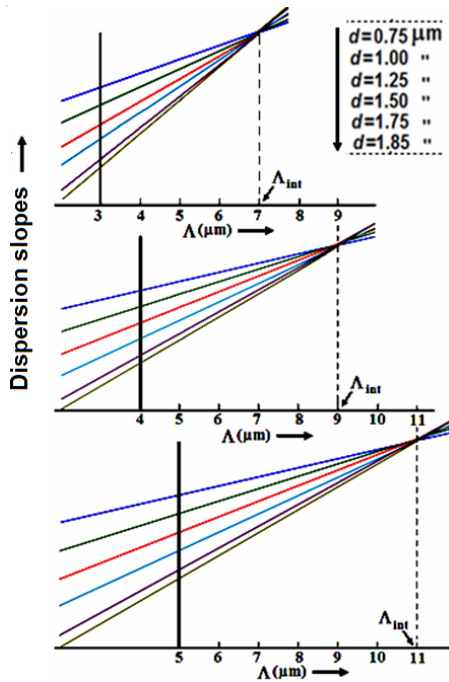
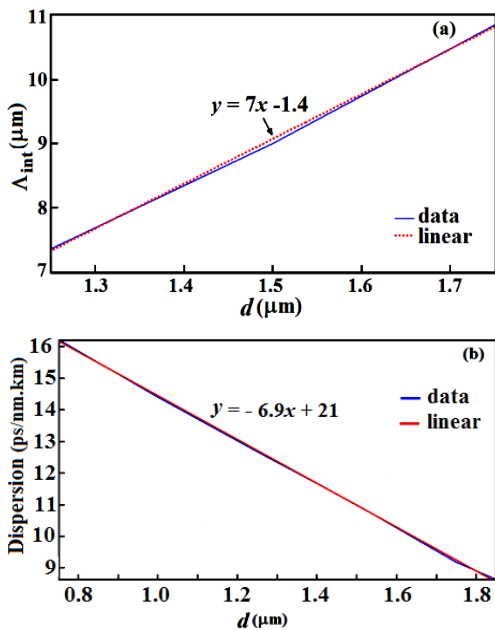
**Figure 7.** Variations of dispersion versus the pitch for various values of  $d$  and  $N = 11$ . (a) at  $\lambda = 0.8 \mu\text{m}$  and (b)  $\lambda = 1.55 \mu\text{m}$

A further investigation on Fig. 7 shows that at and beyond  $\Lambda = 3 \mu\text{m}$ , all the slopes of the dispersions in the calculating range of air-hole diameter  $d$ , intersect at about twice the corresponding value of  $\Lambda$  denoted by  $\Lambda_{\text{int}}$ . In other words, the ratio  $(\Lambda_{\text{int}} / \Lambda)$  almost remain at constant value. For instance, when  $\Lambda = 3, 4,$  and  $5 \mu\text{m}$ , the intersection points  $(\Lambda_{\text{int}})$  of all the dispersion slopes occur at about  $\Lambda_{\text{int}} = 7, 9,$  and  $11 \mu\text{m}$ , respectively, for different values of  $d$ , as shown in Fig. 8.

Also, the relationships between  $\Lambda_{\text{int}}$  and dispersion in terms of the given range of  $d$  vary linearly, defined by equations  $y = 7x - 1.4$  and  $y = -6.9x + 21$ , respectively, at  $\Lambda = 3 \mu\text{m}$  and  $\lambda = 1.55 \mu\text{m}$ , as illustrated in Fig. 9.

**Table 1.** The numerical results obtained in three cases of the PCF designs

Design stage	Air-hole diameter ( $\mu\text{m}$ )	Pitch ( $\Lambda$ ) $\mu\text{m}$	Dispersion at $1.55 \mu\text{m}$	Min. Dispersion at $0.8 \mu\text{m}$	Max. Dispersion at $1.8 \mu\text{m}$	Dispersion slope (deg) at $1.55 \mu\text{m}$
I	0.75	2	14	-70	+22	11
II	1.19	2	9	-47	+15	14
III	0.75	10	20	-100	+34	9

**Figure 8.** Intersection points of dispersion slopes obtained as  $\Lambda_{\text{int}} = 7, 9,$  and  $11 \mu\text{m}$  at  $\Lambda = 3, 4,$  and  $5 \mu\text{m}$ , respectively, for different values of  $d$ **Figure 9.** The linear relationships between (a)  $\Lambda_{\text{int}}$  and (b) the dispersion versus  $d$  at  $\Lambda = 3 \mu\text{m}$  and  $\lambda = 1.55 \mu\text{m}$ 

In the three cases of PCF designs, it is noticed that for the value of the pitch 5 times higher than the first case, the value of maximum negative dispersion has lowered to  $-100 \text{ ps/nm.km}$  and in the given wavelength range, the highest positive dispersion is found to be at about  $34 \text{ ps/nm.km}$ . For this case, the dispersion at  $1.55 \mu\text{m}$  is obtained as  $20 \text{ ps/nm.km}$  with a slope of  $9 \text{ deg}$ . To compare the slope of the three cases, we found that in the third case the dispersion become about  $36\%$  more flattened. The numerical results obtained in three cases are listed in Table 1 for a qualitative comparisons.

## 4. Conclusions

This paper has presented designs of three PCF structures to study the dispersion behavior under impacts of typical geometrical parameters, such as air-hole diameter and the pitch of the proposed PCF structures with respect to the wavelength variations.

In a qualitative comparison in the present study, beside a reasonable compliance, the dispersion variations with respect to higher pitch values are reported, and it is shown that the dispersion could vary linearly as a function of the pitch of the PCF. In addition, it is shown that by knowing the impact of the air-hole diameter on the dispersion variations could benefit the PCF designers for better choices of PCF applications.

Further, it's revealed that in plotting the variations of the dispersion versus wavelength for a typical range of  $d = 0.75 \mu\text{m}$  to  $d = 1.85 \mu\text{m}$ , at  $\Lambda = 2 \mu\text{m}$ , the intersections of dispersion slopes ( $\Lambda_{\text{int}}$ ) of the proposed PCF, with number of air-holes in the cladding  $N = 11$ , varies linearly with air-hole diameter  $d$ . We have also shown that at  $\Lambda = 3 \mu\text{m}$  and  $\lambda = 1.55 \mu\text{m}$ , the relationships between  $\Lambda_{\text{int}}$  and dispersion in terms of  $d$  vary linearly, defined by equations  $y = 7x - 1.4$  and  $y = -6.9x + 21$ , respectively.

Another interesting result worth to note is the flat dispersion spectrum in the range  $1100$  to  $1550 \text{ nm}$ , when  $\Lambda = 2 \mu\text{m}$  and  $d = 1.85 \mu\text{m}$ . Further results showed that the impacts of air-hole diameter  $d$  and the pitch  $\Lambda$  counterbalance each other in a given PCF structure.

---

## REFERENCES

- [1] M.D.Nielsen, C. Jacobsen, N. A. Mortensen, J. R. Folkenberg, H. R. Simonsen, "Low-loss photonic crystal fibers for transmission systems and their dispersion properties", *Opt Exp*, Vol. 12, No. 7, pp. 1372-1376, 2004.
- [2] Md. Selim Habib, Md. Samiul Habib, S. M. Abdur Razzak, Yoshinori Namihira, M.A. Hossain, M.A. Goffar Khan, "Broadband dispersion compensation of conventional single mode fibers using microstructure optical fibers", *Optik- Int. J. Light and Electron Opt.*, Vol. 124, Iss. 19, pp. 3851-3855, 2013.
- [3] S. M. M. Quintero, C. Martelli, A. M. B. Braga, L. C. G. Valente, and C. C. Kato, "Magnetic field measurements based on terfenol coated photonic crystal fibers," *Sensors*, Vol. 11, No. 12, pp. 11103-11111, 2011.
- [4] K. Saitoh, M. Koshiba, "Chromatic dispersion control in photonic crystal fibers: application to ultra-flattened dispersion", *Opt. Exp.*, Vol. 11, No. 8, pp. 843-852, 2003.
- [5] K. Saitoh, M. Koshiba, "Numerical Modeling of Photonic Crystal Fibers", *IEEE J. Lightwave Technol.*, Vol. 23, 3580, 2005.
- [6] Hoo YL, Jin W, Ju J, Ho HL, Wang DN, "Design of photonic crystal fibers with ultra-low, ultra-flattened chromatic dispersion", *Opt. Commun.*, Vol. 242, pp. 327-32, 2004.
- [7] Yan-feng Li, Ching-yue Wang, Ming-lie Hu, A fully vectorial effective index method for photonic crystal fibers: application to dispersion calculation", *Opt. Commun.*, Vol. 238, Iss. 1-3, pp. 29-33, 2004.
- [8] Partha Sona Maji, Partha Roy Chaudhuri, "Supercontinuum generation in ultra-flat near zero dispersion PCF with selective liquid infiltration", *Optik - Int. J. Light and Electron Opt.*, Vol. 125, Iss. 20, pp 5986-5992, 2014.
- [9] M. Samiul Habib, M. Selim Habib, M.I. Hasan, S.M.A. Razzak, "A single mode ultra flat high negative residual dispersion compensating photonic crystal fiber", *Opt. Fiber Technol.*, Vol. 20, Iss. 4, pp 328-332, 2014.
- [10] Maan M. Shaker, Mahmood Sh. Majeed and Raid W. Daoud, "Functioning the Intelligent Programming to find Minimum Dispersion Wavelengths ", *WSEAS Trans. Commnu.*, Vol. 8, Iss. 2, pp. 237-248, 2009.
- [11] Xuyou Li, Pan Liu, Zhenlong Xu, and Zhiyong Zhang, "Design of a pentagonal photonic crystal fiber with high birefringence and large flattened negative dispersion", *Appl. Opt.*, Vol. 54, No. 24, pp. 7351- 7357, 2015.
- [12] Raonaqul Islam, Sohel Rana "Dispersion flattened, low-loss porous fiber for single-mode terahertz wave guidance", *Opt. Eng.*, Vol. 54, No. 5, pp. 055102(1-5), 2015.
- [13] A. Medjouri, L.M. Simohamed, O. Ziane, A. Boudrioua, "Investigation Of High Birefringence And Chromatic Dispersion Management In Photonic Crystal Fiber With Square Air Holes", Accepted, *Optik - International Journal for Light and Electron Optics* 2015, <http://dx.doi.org/10.1016/j.ijleo.2015.05.119>.
- [14] Varshali Sharma and Ritu Sharma, "Design of hybrid photonic crystal fiber with elliptical and circular air holes analyzed for large flattened dispersion and high birefringence," *J. Nanophotonics*, Vol. 10, No. 2, p. 026016, 2016.
- [15] Rakhi Bhattacharya, S. Konar, "Design of microstructure fibers with flat negative dispersion over large wavelength bands", *J. Optoelectron. Advanced Mat.*, Vol. 10, No. 12, pp. 3159-3164, 2008.
- [16] Sejin Lee, Woosung Ha, Jiyoung Park, Soan Kim, Kyunghwan Oh, "A new design of low-loss and ultra-flat zero dispersion photonic crystal fiber using hollow ring defect", *Opt. Commun.*, Vol. 285, Iss. 20, pp 4082-4087, 2012.
- [17] S. K Varshney, N. J. Florous, K. Saitoh, M. Koshiba, T. Fujisawa, "Numerical investigation and optimization of a photonic crystal fiber for simultaneous dispersion compensation over S + C + L wavelength bands", *Opt. Commun.*, Vol. 274, Iss. 1, pp. 74-79, 2007.